Research Article | Vol. 30, No. 25 / 5 Dec 2022 / Optics Express 45592
Optics EXPRESS

Integrated fiber optic spectrally resolved downwelling irradiance sensor for pushbroom spectrometers

CHRISTOPHER GRAHAM,[1] JOHN M. GIRKIN,[1] AND CYRIL BOURGENOT[1,2,*]

[1]Department of Physics, Durham University, Durham DH1 3LE, UK
[2]Precision Optics Laboratory, Durham University, Sedgefield, TS21 3FB, UK
[*]cyril.bourgenot@durham.ac.uk

Abstract: We present an integrated fiber optic spectrally resolved downwelling irradiance sensor for pushbroom hyperspectral imagers. The system comprises of a cosine corrector and custom fiber patch cables, collecting the ambient light in a large solid angle and feeding it directly to the entrance slit of the spectrometer. The system enables simultaneous measurement of downwelling and upwelling irradiance using the main hyperspectral camera sensor. As a demonstration, the spectral reflectance of a soil sample was measured with a RMSE of 8.4%, a significant improvement on the RMSE of 54% found without correction. At a weight of approximately 10 grams, this system provides a substantial weight saving over standalone incident light sensing instruments.

1. Introduction

One of the key challenges to aerial remote sensing is cloud cover, with observations gauging annual cloud cover to be between 66-70%. [1] This heavily impacts traditional high altitude or satellite short wave infrared (SWIR) instruments, as these wavelengths do not penetrate cloud cover. Using small unmanned aerial systems (UAS) that can fly at altitudes far below the cloud ceiling, compact and lightweight hyperspectral imagers can be guaranteed direct line of sight with the ground even on heavily overcast days.

However, operating beneath the cloud ceiling presents its own set of challenges. If the cloud layer is thin or patchy, the downwelling irradiation incident on the ground surface can significantly vary over short timescales, demonstrated in Fig. 1. These variations are spectrally dependant, as the water droplets in the clouds strongly and non-uniformly absorb light in the same wavelength bands used to characterize features such as soil moisture. Accurate measurements of the ground's reflectance are key to measuring accurate soil moisture levels, meaning these variations in incident light levels must be measured and accounted for. [2]

This can be done in several ways. The simplest method is to place reflectance standard panels at set ground control points, which are then overflown by the drone. [3] If several identical panels are placed down and measured, changes in incident light intensity can be calculated and interpolated between the panels. This method can work if lighting conditions in the field are relatively stable, but struggles to completely account for conditions with fast moving cloud cover, often seen in temperate regions.

Another commonly used method for small area UAS surveys is to set up a dedicated ground based spectrometer to continuously measure downwelling irradiance data. [4] This solution provides much higher temporal resolution than reflectance panels, but can be difficult to apply for large survey areas. In sparse cloud cover conditions, the area on the ground affected by a passing

#477699 https://doi.org/10.1364/OE.477699
Journal © 2022 Received 9 Oct 2022; accepted 16 Nov 2022; published 30 Nov 2022

Optics EXPRESS

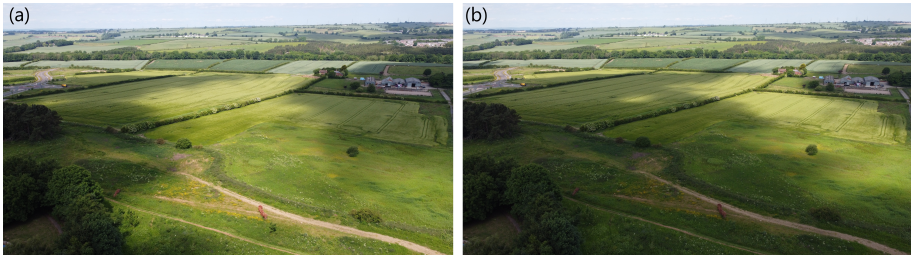

Fig. 1. Example of the non-uniform lighting conditions caused by intermittent cloud cover. Two images recorded 6 seconds apart, using a DJI Mavic Mini.

cloud can be smaller than the survey area, leading to the UAS and the ground system receiving different illumination levels.

This problem can be solved by moving the downwelling irradiance sensor from the ground onto the drone. [5] Generally this is done using a second compact spectrometer mounted to the top of the UAS, fitted with a skyward facing optical diffuser to couple in light from a wide acceptance angle. This enables measurement of downwelling irradiance at the drone position to be monitored continuously. This method does have some trade-offs compared to ground based incident light sensors. Adding an additional spectrometer to the UAS adds weight, power, and packaging complexity, decreasing the possible flight time of the aerial platform, and placing a lower limit on the size of the platform necessary to fly with the instrument. The additional spectrometer also increases the computational load on the low power single board computer used to run and log data from the instruments and the UAS flight computer. The light received by the second spectrometer does not follow the same optical path as the one used for data acquisition, and the sensor used for irradiance measurement is likely to have a different response than the one used to produce the datacube, requiring a separate calibration.

This paper presents a method for measuring common path downwelling irradiance data without the use of additional spectrometers. Using a typical and commonly used pushbroom spectrometer, an integrated fiber optic fed calibration channel has been added to directly measure variations in incident light levels using the same spectrometer camera sensor. By trading off a small portion of the on ground swath width, this design removes the need for the additional spectrometer and associated hardware, along with the additional steps of syncing the spectral and temporal outputs of the two spectrometers. This presents an advance in the capabilities of compact hyperspectral imagers designed for smaller UAS chassis.

2. Optical design

The optical path for this system begins with a cosine corrector, an optical diffuser designed to couple light into a fiber optic cable from an almost 180° hemisphere. This is used to ease coupling of light into the fiber, especially when the angle between the surface normal to the fiber and the Sun is high. The light is then coupled into an ultra low -OH fiber (Polymicro), chosen for its low absorption in the (SWIR) wavelength range. The fibre used has a core diameter of 100 μm, and a numerical aperture of 0.22. The other end of the fiber is positioned at the upper edge of the spectrometer entrance slit. The positioning is set so as to replace the very outermost spatial channels of the camera sensor, which would otherwise image the target through the objective lens, with the light transmitted by the fiber optic. The slit side of the fiber was just simply cleaved, and a small diameter fiber (170 μm) was chosen to limit the number of spatial channels blocked. The field of view loss is approximately 3%, although this could be reduced by further revisions of mounting hardware. A schematic view of the optical system is shown in Fig. 2.

Optics EXPRESS

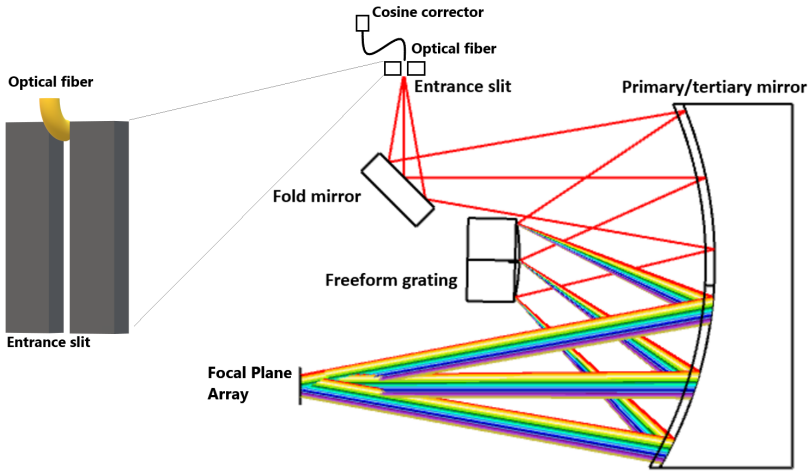

Fig. 2. Schematic overview of the fiber calibration system.

The pushbroom spectrometer uses commercial transmissive imaging fore-optics for compactness, with the two main objectives having focal lengths of 16 mm and 25 mm. [6] The use of these compact lenses results in there being very limited space between the back of the lens assembly and the front of the entrance slit. To secure the fiber into position, a 26 gauge hypodermic needle was cut and shaped, then positioned using a small 3D printed guide. This assembly fits inside of the small adapter plate necessary to attach the C-Mount lenses to the slit. The fiber was threaded through the needle, and secured using a UV cure glue. In total, the entire assembly weighs under 10 grams. Renderings of the system are shown in Fig. 3.

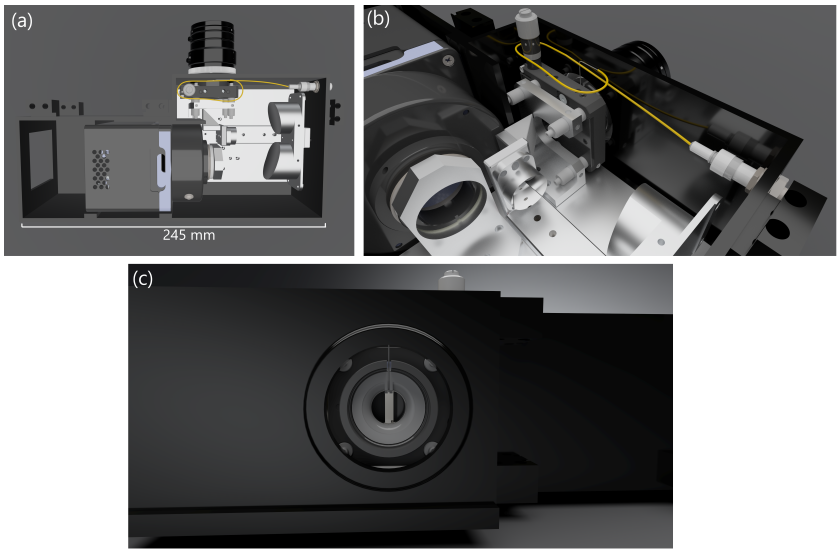

Fig. 3. Rendering of fiber system, showing (a) a wide angle view of the system, (b), a close up of the fiber/needle assembly, and (c), a close up of the needle and mounting plate.

To increase the physical robustness of the setup, crucial for field use with UAVs, a quick disconnect fitting was added. A SMA to SMA mating sleeve was inserted into the instrument

Optics EXPRESS

casing, providing a way to quickly connect to SMA 905 terminated fibers together with minimal coupling loss. The addition of the fiber port means that any stresses or strains caused by snagging of the external fiber do not damage or affect the precise positioning of the internal fiber. The port also enables the external patch cable to be changed out for different lengths depending on the instrument platform being used.

3. Results

To demonstrate the use of the incident light calibration channel, the system was set up outside on a tripod, using a computer controlled rotation stage to provide scanning movement for the hyperspectral imager. A tray of uniformly dry soil was prepared by oven drying a local soil sample, and imaged under both clear and cloudy conditions. For all images the scanning motion is from right to left.

A hyperspectral image of a 50% reflectance reference panel was also captured. This can be used to correlate the signal from the fiber channel to a reference standard, enabling the data to be used to calculate reflectance. It also enables the fiber correction method to be compared to the standard panel measurement method.

Measurements of dry soil under cloudy conditions are shown in Fig. 4. Figure 4(a) shows the measured reflectance map at 1220 nm, calculated using an earlier measurement of a reflectance standard panel under clear conditions as a reference. As the image of the dry soil was taken under changing illumination conditions, the soil reflectance at the right of the image is calculated as having significantly lower value than the soil at the left of the image, despite the soil being of uniform moisture content. Without knowledge of incident light intensity, it is impossible to distinguish between reduced incident light levels and a truly darker material. Figure 4(b) shows a reflectance map of the same soil sample, this time corrected for varying illumination using the fiber optic calibration channel. Note that the resulting reflectance map is much more uniform in appearance. Comparing the corrected mean soil reflectance spectrum with reflectance recorded under clear skies, the percentage root mean square error (RMSE) was found to be 8.4%. When using the HIAM [7] method for recovering soil moisture content, this results in a 10% increase in predicted absolute gravimetric soil moisture content compared to measurements made under clear conditions. [7] Performing the same analysis with the uncorrected reflectance data, the mean spectral RMSE was 54%, which results in the soil sample's moisture content being overestimated by 58%.

The dynamic range and signal to noise ratio of the camera limits the range of light intensities that can be corrected for. If the incident light intensity drops too low for the camera's settings, noise will dominate the measured signal from both the main lens and the fiber channel. An example residual map calculated at 1220 nm is plotted in Fig. 4(c), showing that the highest residuals were found in the areas covered by the darkest of clouds. Under these conditions, better results could be obtained by using the fibre as a light meter to guide an auto-exposure algorithm, varying exposure to compensate for changing levels of illumination.

The data from the calibration fibre also demonstrates the need for spectrally resolved calibration methods. Figure 4(d) shows the normalised intensity from two spectral bands plotted with time as a cloud passes. Light at 1040 nm wavelength is further from a water absorption band than that at 1540 nm wavelength, and so is less absorbed by passing cloud cover. Light metering methods based on averaging over larger wavelength ranges could under estimate reflectance at some wavelengths by 10%.

Rotating the camera upwards 90° to face horizontally, some landscape images were taken under the same cloudy conditions. An example image of a grassy field and trees is shown in Fig. 5(a). This image, shown at 1220 nm, was captured using a right to left scan direction with a 20 second duration. During this time a slim break in the cloud cover was moving across the field towards the camera. This can be seen in Figs. 5(b) and (c), which show RGB images of the field at the

Optics EXPRESS

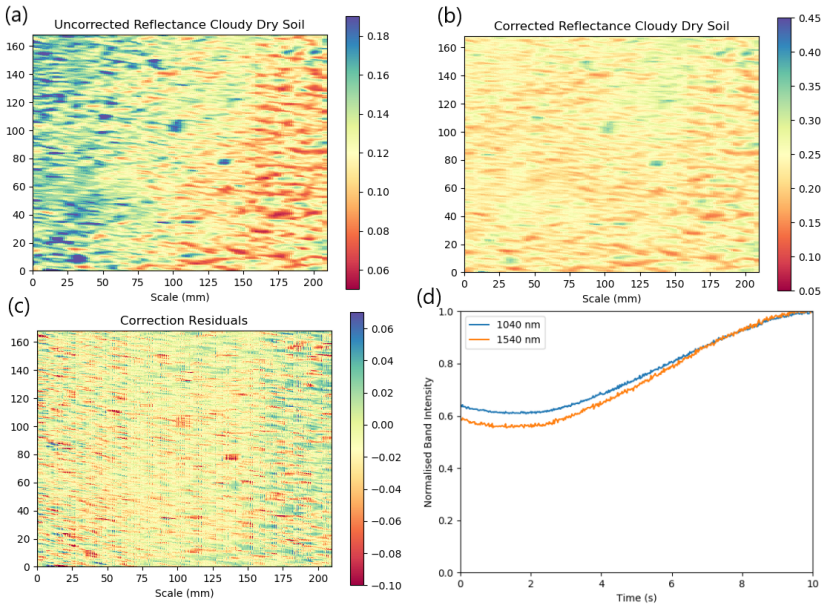

Fig. 4. (a) Uncorrected reflectance measurement of uniform dry soil as cloud passes by. Note the measured reflectance values for the right of the image vary significantly from the left. Reflectance units normalised to white Spectralon panel.(b) Reflectance measurements corrected for changing illumination using fibre. (c) Measured reflectance residuals after correction. Calculated by comparing measurements of the same sample taken under cloudy and clear conditions. The highest residuals correspond to the thickest cloud cover. (d) Normalised incident light intensity as measured using the fibre for two wavelengths as cloud passes through. See Visualization 1 for an animated version including concurrent RGB drone and ground footage.

beginning and end of the scan, with the exposure settings of the camera held constant. From these images, it is possible to see the bright band of sunlight moving towards the camera. When combining this moving lighting with the pushbroom scan acquisition of the hyperspectral imager, the result is a curved streak of higher intensity seen in the end image. An animated scanning plot, along with concurrent RGB drone and ground based imagery showing these effects can be seen in Visualization 1, while Visualization 2 better illustrates the movement of the cloud seen in 5(b) and (c). By using wind velocity measurements at the cloud altitude level, it may be possible to correct for this striping, especially if caused by a single cloud. However, on days where cloud cover is made up of several layers each moving a different speeds, accurate correction may prove difficult. These difficulties apply in particular to scenes where a large horizontal depth is imaged, and should not relate to scenes imaged using a nadir facing sensor on a moving platform, as is the case for most airborne remote sensing applications.

Optics EXPRESS

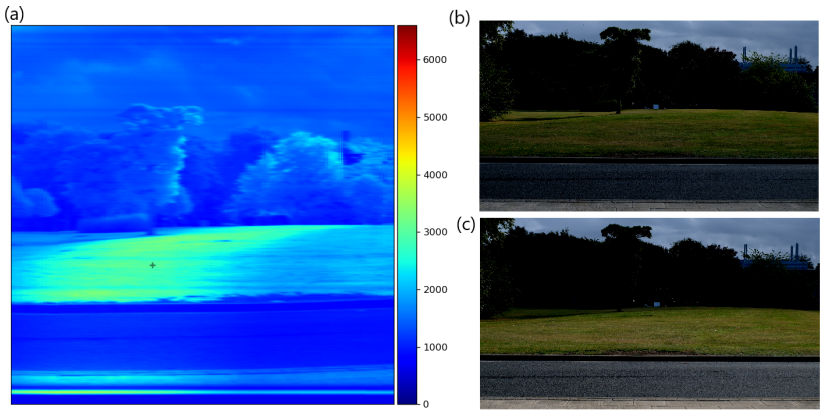

Fig. 5. (a) Raw camera signal map for an image taken over a field during intermittent cloud. Image recorded at 1220 nm, with a right to left scan direction with a duration of 10 seconds. Curved bright area is due to cloud cover movement towards the camera. (b) and (c) are RGB images corresponding to start and finish of the scan. For these two images, the camera exposure settings were kept constant. Note the movement of the bright area from high depth in (b) to low depth in (c), resulting in the curved band seen in (a). See Visualization 2 for an animated version of (b) and (c).

Optics EXPRESS

4. Conclusion

In summary, the design and demonstration of a fiber optic spectrally resolved downwelling irradiance sensor integrated into a compact hyperspectral imager has been presented. The system makes use of an optical fiber assembly to directly measure incident illumination levels using the main camera sensor, enabling simultaneous spectral measurements of downwelling and upwelling light. This information can be used to calculate true target reflectance factors under solar illumination, even under changeable cloud cover. By making use of the main camera sensor, rather than a standalone compact spectrometer, the weight of the calibration system was kept below 10 grams. The performance of the system was demonstrated using a local soil sample, showing reflectance measurements taken of dry soil under both cloudy and clear conditions. Without correction, reflectance measurements of soil samples produced moisture content estimates 60% above the true gravimetric value. By correcting the reflectance data using the calibration channel, this can be brought down to an over estimate of around 10%. This could be improved further by adding an auto-exposure system guided by the calibration data, improving signal to noise ratio under changing cloud cover.

Funding. Engineering and Physical Sciences Research Council (EP/S001727/1).

Acknowledgments. This work was supported by an UKRI- EPSRC Innovation fellowship "A compact novel hyperspectral imager for more reliable and precise agriculture" - EPSRC Grant Reference : EP/S001727/1

Disclosures. The authors declare no conflicts of interest.

Data availability. Data underlying the results presented in this paper are not publicly available at this time but may be obtained from the authors upon reasonable request.

References

1. K. Mao, Z. Yuan, Z. Zuo, T. Xu, X. Shen, and C. Gao, "Changes in Global Cloud Cover Based on Remote Sensing Data from 2003 to 2012," Chin. Geogr. Sci. **29**(2), 306–315 (2019).
2. C. J. Köppl, R. Malureanu, C. Dam-Hansen, S. Wang, H. Jin, S. Barchiesi, J. M. Serrano Sandí, R. Mu noz-Carpena, M. Johnson, A. M. Durán-Quesada, P. Bauer-Gottwein, U. S. McKnight, and M. Garcia, "Hyperspectral reflectance measurements from UAS under intermittent clouds: Correcting irradiance measurements for sensor tilt," Remote. Sens. Environ. **267**, 112719 (2021).
3. H. Aasen and A. Bolten, "Multi-temporal high-resolution imaging spectroscopy with hyperspectral 2D imagers – From theory to application," Remote. Sens. Environ. **205**, 374–389 (2018).
4. A. Burkart, S. Cogliati, A. Schickling, and U. Rascher, "A novel UAV-Based ultra-light weight spectrometer for field spectroscopy," IEEE Sens. J. **14**(1), 62–67 (2014).
5. J. Suomalainen, T. Hakala, R. A. de Oliveira, L. Markelin, N. Viljanen, R. Näsi, and E. Honkavaara, "A novel tilt correction technique for irradiance sensors and spectrometers on-board unmanned aerial vehicles," Remote Sens. **10**(12), 2068 (2018).
6. C. Graham, J. M. Girkin, and C. Bourgenot, "Freeform based hYperspectral imager for MOisture Sensing (FYMOS)," Opt. Express **29**(11), 16007–16018 (2021).
7. C. Graham, J. Girkin, and C. Bourgenot, "Spectral index selection method for remote moisture sensing under challenging illumination conditions," Sci. Rep. **12**(1), 14555 (2022).